

PAPER

Plasma-assisted abatement of SF₆ in a packed bed plasma reactor: understanding the effect of gas composition

To cite this article: Xiaoxing ZHANG *et al* 2020 *Plasma Sci. Technol.* **22** 055502

View the [article online](#) for updates and enhancements.

Plasma-assisted abatement of SF₆ in a packed bed plasma reactor: understanding the effect of gas composition

Xiaoxing ZHANG (张晓星)^{1,2,3}, Yuan TIAN (田远)¹, Zhaolun CUI (崔兆仑)^{1,3}
and Ju TANG (唐炬)¹

¹ School of Electrical Engineering and Automation, Wuhan University, Wuhan 430072, People's Republic of China

² School of Electrical and Electronic Engineering, Hubei University of Technology, Wuhan 430068, People's Republic of China

E-mail: xiaoxing.zhang@outlook.com and Zhaoluncui@163.com

Received 21 September 2019, revised 25 December 2019

Accepted for publication 26 December 2019

Published 12 February 2020



Abstract

The potential impact of SF₆ as a potent greenhouse gas on the global climate is highly attractive. This paper studies the effect of H₂O concentration, SF₆ inlet concentration and pre-heating temperature on SF₆ abatement in a packed bed plasma reactor in terms of the removal efficiency and products selectivity. The results showed that the best performance in SF₆ abatement was obtained at 1% H₂O and 100 °C with 98.7% destruction and remove efficiency (DRE) at 2% SF₆. Higher energy yields was obtained under higher SF₆ inlet concentration. Moreover, the existence of water vapor weakened the micro-discharge and provided H and OH radicals for this system, which showed a close relationship to removal efficiency and products selectivity. Among four sulfur-containing products, SO₂F₂ was more stable than SOF₂, SOF₄ and SO₂. Meanwhile, SOF₄ and SO₂ were very susceptible to the above parameters. This article provides a better understanding of SF₆ abatement in a view of both scientific and engineering.

Keywords: SF₆, PBR, plasma, gas composition

(Some figures may appear in colour only in the online journal)

1. Introduction

Sulfur hexafluoride (SF₆) is a potent greenhouse gas with extremely stable chemical properties. Research has showed that its global warming potential (GWP) is 23 000 times that of carbon dioxide (CO₂), which could exist for more than 3200 years in the atmosphere [1–3]. Meanwhile, SF₆ has been widely applied to the power industry, semiconductor and metallurgy sectors due to its excellent dielectric strength, arc-extinguishing properties and chemical inertness. Recently, the potential impact on the global climate has attracted tremendous attention. Nowadays, more than 10 000 tons of SF₆ are produced every year, over 80% of which are used in gas-insulated switchgears [4]. However, green insulating gas still

should be further studied, which means that humans will face the problem of SF₆ treatment for a long time [5, 6]. For instance, the SF₆ issues would appear when the equipment was broken or repaired. In addition, the concentration of SF₆ applied to semiconductor sectors and the metallurgy industry is usually extremely low, which is difficult for recycling. Those problems pose serious hazards to the ecological system. Therefore, how to abate SF₆ waste gas has become a hot issue in the industrial environmental protection field.

Compared with traditional methods, such as pyrolysis and photolysis, no-thermal plasma (NTP) technology has exhibited high potential in addressing environmental pollutants due to the presence of abundant energetic electrons and chemical reactive species [7–15]. Dielectric barrier discharge (DBD), as one of the methods, has the advantage of generating NTP compared with other types of discharge

³ Authors to whom any correspondence should be addressed.

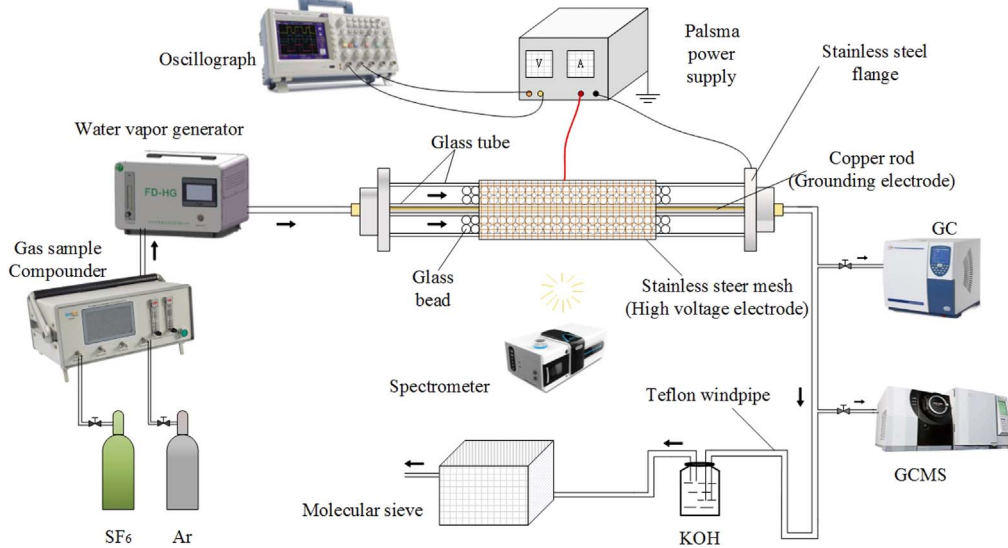


Figure 1. Schematic of the experimental setup.

approaches due to the simplicity and scalability of its experimental setup [16]. In DBD plasma, free electrons are highly energetic with a typical electron energy of 1–10 eV, which is sufficient to activate reactant molecules (SF_6) to produce chemically reactive species for the initiation and propagation of chemical reactions arising from the radical chain mechanism [17]. Furthermore, it is worth noting that the overall gas temperature of the DBD can be as low as room temperature and less heat loss can be achieved. Therefore, it has been widely applied to the treatment of industrial waste gas including volatile organic compounds (VOCs) and greenhouse gases [18–23].

However, the plasma behavior is still poorly understood owing to the influence of so many processing parameters on its performance. Much research on this issue has been studied and many enlightening conclusions are obtained. For example, research showed that some packing materials in the reactor could intensify the micro-discharge and surface discharge in the system, and finally the removal efficiency was improved [24–29]. A packed-bed plasma reactor was applied (PBR, DBD with packing materials) to abate SF_6 and CF_4 [29]. The results showed that PBRs exhibited a higher energy efficiency than traditional DBD reactors, which was easier to remove waste gas molecules. Furthermore, studies showed that gas composition also has a huge impact on the SF_6 treatment. Zhang *et al* found that water vapor, oxygen and ammonia (NH_3) could promote the degradation of SF_6 in DBD reactors [30–32]. The above studies are very crucial and the results are very instructive. However, until now, few studies were focused on the combination of packing materials and gas composition.

Water, as a common substance, can be obtained easily. Research demonstrated that lots of H and OH radicals could be generated by water vapor in the plasma area, which can react with those dissociative fragments resulting from the decomposition of SF_6 and help to remove SF_6 [31]. However, the influence of water vapor concentration on the degradation

process has not been investigated comprehensively, as well as its effect on the by-products. Many researchers have studied the impact of different applied gases on products selectivity, but the influence of the concentration of the applied gases on products selectivity was ignored. Investigation into the products concentration and selectivity under different conditions provides a better point of view to understand the effect of those parameters on SF_6 abatement. Furthermore, this work also could provide ideas of the treatment of other exhaust gases.

In this study, the removal of SF_6 was conducted in a PBR using argon (Ar) as a carrier gas. The influence of different plasma processing parameters (water vapor concentration, SF_6 inlet concentration and pre-heating temperature) on removal efficiency and products selectivity of SF_6 was investigated comprehensively.

2. Experiment

2.1. Experimental setup

The experiments were performed in a glass beads packed bed, non-thermal atmospheric pressure plasma reactor, which was shown schematically in figure 1. The experimental setup consisted of a gas source, a plasma generator, detecting equipment and exhaust gas treatment modules. The gas source was applied to supply particular gas composition of the system including water vapor generator (FD-HG, Furande, Suzhou, China), Gas sample compounder (GC500, Tunkon Electrical Technology Co., Ltd), SF_6 and Ar (above 99.999%, Newradargas Co., Ltd, Wuhan). The H_2O concentration was measured by a mirror dewpoint meter (GE600, Henan Relations Co., Ltd). The water vapor generator contained a heating module inside, which could preheat the gas input from the gas distributor. Ar was the carrier gas, which brought SF_6 and

Table 1. The physical and chemical properties of the four products [30].

Products	Melting point (°C)	Boiling point (°C)	Chemical properties
SOF_4	-120	-55.4	Hydrolysis produces SO_2F_2 and HF
SOF_2	-130	-43.8	Hydrolysis produces HF and SO_2
SO_2	-72.7	-10	Reaction with lye
SO_2F_2	-55	29	Resistant to hydrolysis even up to 150 °C

water vapor into the reactor and then went through detecting apparatus.

The power supply (CTP-2000K, Nanjing Suman Electronics) was applied to change the single-phase electric supply into high frequency and high voltage alternative currency and applied it on the reactor to generate plasma. The discharge reactor employed in the present work was a coaxial cylindrical reactor. A stainless-steel mesh (high-voltage electrode) was wrapped tightly around a quartz tube with an external diameter of 24 mm and an inner diameter of 20 mm. The inner ground electrode was a copper rod with an external diameter of 4 mm, which was installed along the axis of the quartz tube. The discharge length was about 200 mm with a discharge gap of 6 mm, the thickness of the quartz barrier layers inside and outside the reactor was 2 mm. Glass beads with a diameter of 2.5 mm were filled in the reactor as the packing material.

Detecting equipment included an oscilloscope (Tektronix TDS 320), emission spectrometer (MX2500+, Ocean Optics Co., Ltd, USA), gas chromatograph (GC, GC-450, Shanghai Huishi Instrument) and gas chromatography-mass spectrometry (GCMS, Shimadzu Ultra 2010 plus with CP-Sil 5 CB column, SHIMADZU Co., Ltd). The oscilloscope was applied to record the applied voltage and discharge currency of the PBR. The SF_6 concentration before and after treatment was detected by GC. The emission spectrometer was a three-channel one in which a grating was used as a beam splitting element and a CCD array as a beam splitting element detector. It could measure the wavelength from 300 nm to 800 nm with 0.1 nm optical resolution. Four kinds of sulfur-containing byproducts were quantitatively detected by GCMS.

The exhaust gas processed module included lye and a molecular sieve. The water-soluble products (SOF_4 , SOF_2 , SO_2) were absorbed by the lye, while the remaining water-insoluble product (SO_2F_2) was adsorbed by the molecular sieve [33–35]. The properties of the four products are shown in table 1.

The experiment conditions were summarized as follows: the input power was fixed at 100 W, the electric source frequency was fixed at 8.7 kHz, the mixed gas flow rate was determined to be 150 ml min^{-1} , all tests were conducted at room temperature (298 K) under atmosphere pressure (101.3 kPa). Additive water vapor flow rate was $0.15\text{--}3 \text{ ml min}^{-1}$ (the water vapor concentration was corresponding 0.1%–2%), the concentration of SF_6 ranged from 1% to 8%. Each set of experiments was performed three times.

2.2. Measurement

The destruction and removal efficiency (DRE) was calculated as follows:

$$\text{DRE}(\%) = \frac{c_{\text{in}} - c_{\text{out}}}{c_{\text{in}}} \times 100\% \quad (1)$$

where c_{in} and c_{out} (ppm, parts per million) refers to the SF_6 concentration before and after treatment respectively.

Energy yield (EY) was defined as the mass (g) of SF_6 degradation per unit of energy (kWh). It was calculated as follows:

$$\text{EY(g kWh}^{-1}) = \frac{m_{\text{SF}_6}}{P_{\text{in}}} \times 10^3 \\ = \frac{\text{DRE} \times c_{\text{in}} \times v_g \times 60 \times 146}{22400 \times P_{\text{in}}} \times 10^3 \quad (2)$$

where m_{SF_6} denotes the mass of SF_6 abated in unit time (h). P_{in} refers to the input power (W) of the power supply. v_g refers to the velocity (ml min^{-1}) of the mixed gas.

S_K (selectivity) is the selectivity of a particular byproduct (K), where c_K refers to the byproduct concentration.

$$S_K(\%) = \frac{c_K}{c_{\text{in}} - c_{\text{out}}} \times 100\%. \quad (3)$$

3. Results and discussion

3.1. Removal efficiency

Figure 2 presents the DREs and EY as a function of water vapor concentration, SF_6 inlet concentration and pre-heating temperature. In figure 2(a), the DRE of 2% SF_6 increased first and then dropped slightly. This tendency indicated that there was an optimal water vapor concentration range contributing to the promoted effect on DRE at 2% SF_6 in the system. Moreover, figure 2(b) shows that the DREs decreased as the SF_6 concentration decreased. But the DRE in the 1% H_2O group was always higher than that of the 2% H_2O group. It suggested that higher SF_6 concentration had an adverse effect on DRE. Furthermore, a better promoting effect on DRE was achieved in 1% group compared with the 2% H_2O group under the same conditions. Figure 2(c) demonstrates the DRE as a function of pre-heating temperature. Compared with figure 2(a), warming up the mixed gas before discharge was beneficial to the abatement of SF_6 obviously. The 3% difference of the highest DRE was obtained before and after pre-heating. However, a negligible tendency began to be observed as the pre-heating temperature raised up to 120 °C.

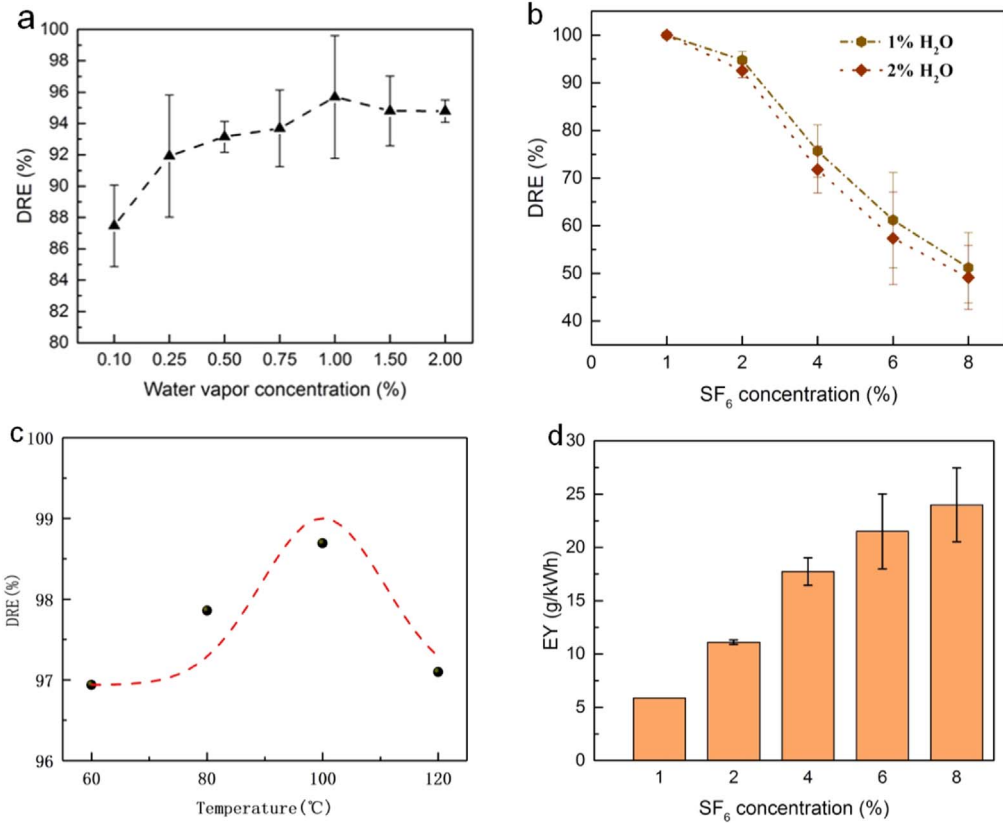


Figure 2. (a) DRE under different water vapor concentrations (2% SF₆, 100 W, 150 ml min⁻¹), (b) DREs under different SF₆ inlet concentrations (100 W, 150 ml min⁻¹), (c) DRE at different pre-heating temperatures (2% SF₆ + 1% H₂O, 100 W, 150 ml min⁻¹), (d) EY under different SF₆ inlet concentrations (1% H₂O, 100 W, 150 ml min⁻¹).

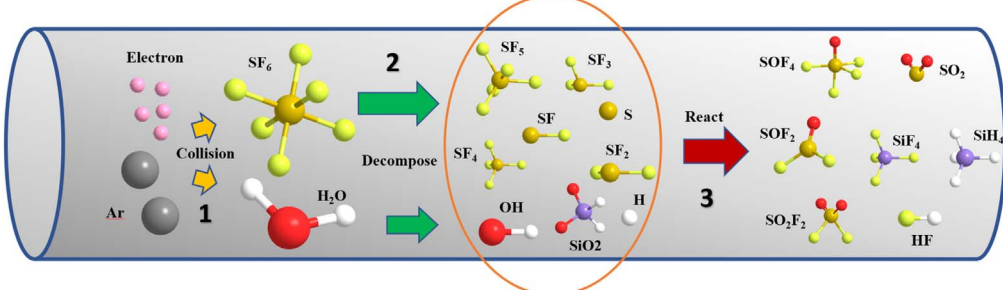


Figure 3. SF₆ degradation process.

Figure 2(d) shows that the EY increased from 5.87 g kW⁻¹h⁻¹ to 24.01 g kW⁻¹h⁻¹ as the concentration of SF₆ increased. It implies that the application of higher SF₆ concentration made better use of energy.

Similar conclusions have been obtained in previous reports. For example, in [30], Zhang *et al* suggested the DRE could increase first and then decrease with the increment of NH₃ concentration. Chen *et al* demonstrated that DRE could decrease with the increment of SF₆ inlet concentration [10]. Based on our previous work, the SF₆ removal process was divided into three parts as shown in figure 3 [32].

Three parts occurred during the treating process including collision, decomposition and reaction [32]. The first step happens first because it provides raw materials for the latter

reactions. Actually, collision consists of the preparation of excited atoms (equation (4)) and free electrons. The reaction threshold will be lower because of those reactive species. Then, with the increment of the electric field, those particles will speed up to obtain high energy. When they collided with SF₆ or H₂O molecules, those molecules will be decomposed into SF_x, OH and H, as the equations (5)–(7) show. In this paper, Ar was used as carrier gas because it can generate lots of free electrons by the Penning ionization (references [1] and [36] reported this effect). After this stage, those products will recombine to generate SF₆ again if there is no intervention (equation (8)). However, those radicals will react with SF_x because they are very active in the plasma region. Therefore, the existence of H, OH can inhibit this reverse reaction. In this

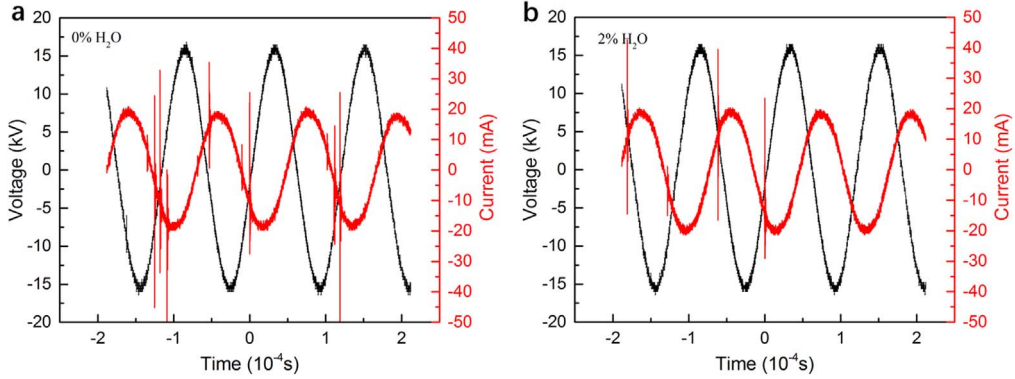
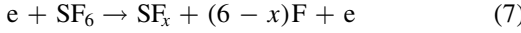
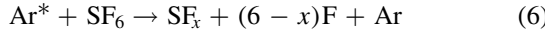
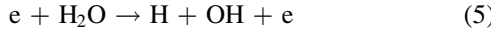


Figure 4. (a) The applied voltage and current waveform of the PBR under no H₂O (2% SF₆/Ar, 100 W, 150 ml min⁻¹), (b) the applied voltage and current waveform of the PBR under 2% H₂O concentration (2% H₂O + 2% SF₆, 100 W, 150 ml min⁻¹).

way SF₆ can be abated completely.



When the water vapor was lower than 0.25%, DRE climbed quickly with the increment of water vapor concentration. However, when the water vapor concentration continued to increase, this promoted effect slowed down and even disappeared. When the water vapor concentration was 2%, the DRE was a litter lower than that of 1% H₂O. However, a higher DRE was still obtained compared with the situation of no H₂O. This result is in accordance with that by Lee *et al* [13]. It clearly indicated that there was a tradeoff between the positive and adverse influence of H₂O. Firstly, water vapor can prevent sub-fluoride recombination, which was helpful to improve the DREs and EY. However, water vapor was also an electronegativity gas. It can absorb free electrons in the ambient, which will weaken collision and decomposition. References [13] and [37] also reported the similar conclusion that the highest removal efficiency has been obtained under an optimized amount of oxygen condition. However, the oxygen concentrations were not same in the two pieces of research, which may be due to the difference between their working conditions. Therefore, the optimized H₂O concentration of plasma application is determined by the specific work conditions rather than a fixed value.

Figure 2(b) shows DREs as a function of SF₆ concentration. Similar to water vapor, SF₆ is also an electronegativity gas, high concentration of SF₆ could suppress the development of micro-discharge and lower the DRE. Therefore, its DRE dropped from 100% at 1% SF₆ to 51.2% at 8% SF₆. Moreover, 1% of the H₂O group had a better abatement efficiency, which indicated that it has a better tradeoff in this system. The degradation efficiency of SF₆ was improved when H₂O concentration between 0.10% and 0.25% was added. In addition, it is easy to understand that the DRE increased under higher temperatures as higher temperatures led to extensive molecules movement and intensified

collisions between reactive species. However, if the temperature continued to increase, opposite results would occur because the higher temperatures will enlarge the volume of mixed gas, leading to the increased flow rate and the decreased average residence time, and this effect decreased the DRE [17]. As shown in figure 2(d), the total mass of SF₆ treated will increase with the SF₆ concentration. In [30], Zhang *et al* pointed out that the mass of degraded SF₆ increasing with flow rate, because the increased flow rate and concentration would lead to the increment of the number of SF₆ molecules. This effect would also appear when the SF₆ inlet concentration increased because both bring more SF₆ molecules into the reactor. When the concentration of SF₆ was low, the averaged number of collisions of the SF₆ molecule was higher, thus leading to more sufficient degradation of SF₆ molecules (higher DRE), but the total amount of degradation was less (lower EY). In contrast, the averaged number of collisions of the SF₆ molecule decreased, although the degradation was not sufficient (lower DRE), more molecules participated in the reaction (higher EY). Therefore, the increment of SF₆ concentration would also increase the SF₆ degradation. The above investigation revealed that increasing SF₆ concentration was a feasible method to improve EY.

Similar voltage and current amplitude are shown in figure 4, which implies that the addition of water vapor will not change the electric parameter of the system. However, it can be found that the number of micro-discharge channels is quite different. The intensity of the micro-discharge can reflect the movement of charged particles in the air gap [36]. Under a higher humidity environment, the micro-discharge in the tube was much less than the group without water. Because water molecules can adsorb free electrons during the process of ionization. This process will result in lower energy applied to the SF₆ decomposition due to the finite total energy. Consequently, the micro-discharge was difficult to happen, thus decreasing the number of discharge pulse.

When the kinetic energy of a free electron colliding with an atom or molecule is greater than their excitation energy, they will be excited and corresponding characteristic spectra were also emitted. The active substances involved in the reaction can be studied by these lines, as shown in figure 5. In this paper, quartz glass was applied as a barrier medium to

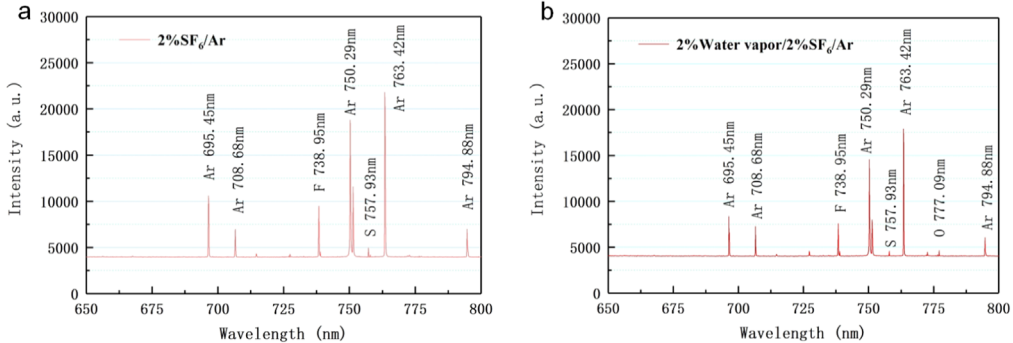


Figure 5. (a) Emission spectrum ($2\% \text{ SF}_6$, 100 W , 150 ml min^{-1}), (b) emission spectrum. ($2\% \text{ SF}_6 + 2\% \text{ H}_2\text{O}$, 100 W , 150 ml min^{-1}).

collect the emission spectrum. By comparing with the NIST database [38], several main atomic lines of the Ar/SF₆ as well as Ar/SF₆/H₂O plasma emission spectra were initially diagnosed (Ar 695.45 nm, Ar 708.68 nm, Ar 750.29 nm, Ar 794.88 nm, F 738.95 nm, S 757.93 nm, O 777.09 nm). Among them, the intensity of Ar lines was much greater than those of other elements, because argon was the main component of the mixed gas. A previous study demonstrated that the kinetic energy of free electrons was as high as 11.5 eV in the DBD system, which could excite argon atoms in the mixed gases [23]. Moreover, both F and S atoms appeared in the emission spectrum due to the break and decomposition of many SF₆ molecules under plasma conditions, and the emission intensity of F was much larger than S. Firstly, the number of F atoms was more than S atoms; Secondly, a single S atom can appear only when the SF₆ molecule was completely decomposed. Furthermore, O was not detected under anhydrous conditions, but a weak line was observed under 2% H₂O, indicating that water molecules were also involved in the decomposition of SF₆. H₂O and SiO₂ were two sources of O in the 2% H₂O system. However, in the anhydrous system, the O atoms could only be obtained from the SiO₂ (etching reaction) [31]. The emission line of the O atoms did not appear in the system, which may be due to the slow progress of the etching reaction. In addition, the intensity of the emission spectrum decreased significantly after the addition of water vapor, evidenced by the intensity of the overall emission spectrum. A similar phenomenon was also found from previous research [39], in which the CO₂⁺ emission spectrum intensity in pure CO₂ was much smaller than that of the diluted gas. Therefore, this phenomenon may be due to the absorption of more electrons and energy by the H₂O as mentioned above (equations (9)–(12)). Its adsorption capacity for free electrons was strong although the moisture was relatively low, and this adsorption may induce decreased energy for exciting Ar atoms and made the intensity of Ar lines descend.

3.2. Products analysis

Figure 6 presents the concentration and selectivity of four products as a function of water vapor concentration. As shown in figure 6(a), the concentration of SOF₂ decreased dramatically while SO₂ content went up significantly as the

water vapor concentration increased from 0.1% to 2%. In addition, the other two products were relatively stable. Clearly, among the four products, SO₂ and SOF₄ were sensitive to water vapor concentration, the concentration of SO₂ increased from 2613.6 ppm to 8543.7 ppm and the concentration of SOF₄ dropped from 790.9 ppm to only 8.6 ppm, respectively. In addition, [31] showed that 0.5% H₂O could significantly enhance the selectivity of SO₂, which is consistent with the results from this paper. However, there is a big difference in the selectivity of SOF₄. This may be due to the higher energy in the PBR system, which led to the inability of the primary product SOF₄ to exist in large quantities. Furthermore, [37] showed that SO₂F₂ kept stable when the O₂ concentration changed, but the SOF₂ decreased significantly. This may be due to the different sensitivity of SOF₂ to H₂O and O₂.

Equations (13)–(18) indicate that the concentration of SF_x should decrease with the increment of x . This will result in a higher concentration of SOF₄ compared with the SOF₂ because the raw materials of the former are much abundant than that of SOF₂ (equations (19)–(22)) [1]. By contrast, figure 6(a) shows the opposite trend. It implied that most of the SOF₄ would react further to be transformed into other substances, as equations (23) and (24) display. When the water vapor concentration was 0.1%, the concentration of SOF₄ was 790.9 ppm; but the concentration of SOF₄ dropped to only 8.6 ppm as the concentration of water vapor increased to 2%. This fact demonstrated that water vapor exhibited a strong suppression effect on SOF₄. That may be due to the fact that H₂O could react with SOF₄ to form SOF₂ and SO₂F₂.

The concentration of SOF₂ cannot fluctuate largely compared with SOF₄. When the water vapor concentration was 0.1%, the concentration of SOF₂ was 3451.8 ppm with the lowest value. Furthermore, when H₂O concentration increased to 0.75%, the highest concentration of 4136.0 ppm for SOF₂ was achieved. Equations (21)–(26) reveal that H₂O has a double effect on SOF₂ concentration because it is not only a reactant to form SOF₂, but a reactant to consume its raw materials. Therefore, when the water vapor concentration was higher than 0.75%, SOF₂ started to decrease.

Similar to SOF₂, the SO₂F₂ increased first and then decreased with the H₂O concentration. The lowest SO₂F₂ concentration value of 4811.9 ppm was achieved when 0.1% concentration of the water vapor concentration was applied.

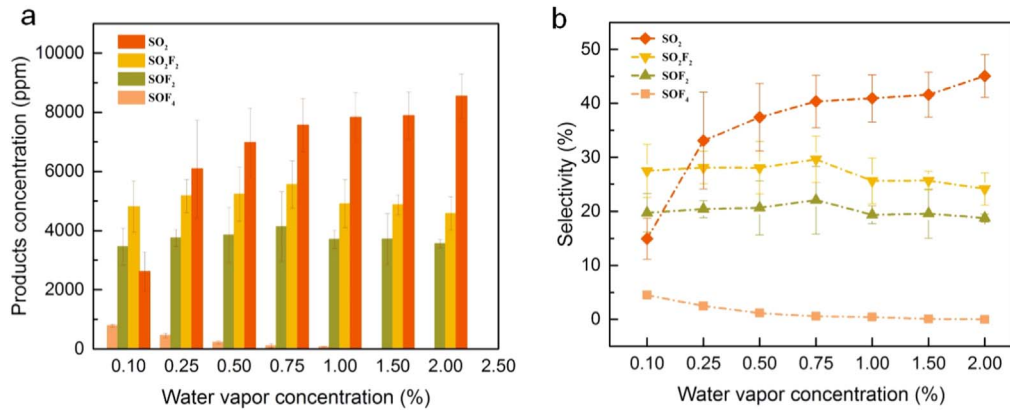


Figure 6. (a) Product concentration under different water vapor concentrations (2% SF₆, 100 W, 150 ml min⁻¹), (b) product selectivity under different water vapor concentrations (2% SF₆, 100 W, 150 ml min⁻¹).

Table 2. Formulas in the degradation process [1, 30].

No.	Reaction	Reaction heat (kcal mol ⁻¹)
(9)	e + H ₂ O → H + OH ⁻	96.64
(10)	e + H ₂ O → H ₂ O ⁻	32.66
(11)	e + H ₂ O ⁻ → OH + H + 2e	84.68
(12)	e + H ₂ O → H ₂ + O + e	197.07
(13)	SF ₆ → SF ₅ + F	86.09
(14)	SF ₅ → SF ₄ + F	41.46
(15)	SF ₄ → SF ₃ + F	97.15
(16)	SF ₃ → SF ₂ + F	53.32
(17)	SF ₂ → SF + F	86.18
(18)	SF → S + F	113.79
(19)	SF ₅ + OH → SOF ₄ + HF	4.51
(20)	SF ₄ + OH + F → SOF ₄ + HF	-156.64
(21)	SF ₃ + OH → SO ₂ F ₂ + HF	-107.59
(22)	SF ₂ + OH + F → SOF ₂ + HF	-160.91
(23)	SOF ₄ + H ₂ O → SO ₂ F ₂ + HF	-26.35
(24)	SOF ₄ + 2H → SOF ₂ + 2HF	—
(25)	SOF ₂ + H ₂ O → SO ₂ + 2HF	-18.33
(26)	SO ₂ F ₂ + 2H → SO ₂ + 2HF	—
(27)	SiO ₂ + 8H → SiH ₄ + 2H ₂ O	—
(28)	SiO ₂ + 4HF → SiF ₄ + 2H ₂ O	—
(29)	S + 2O → SO ₂	—

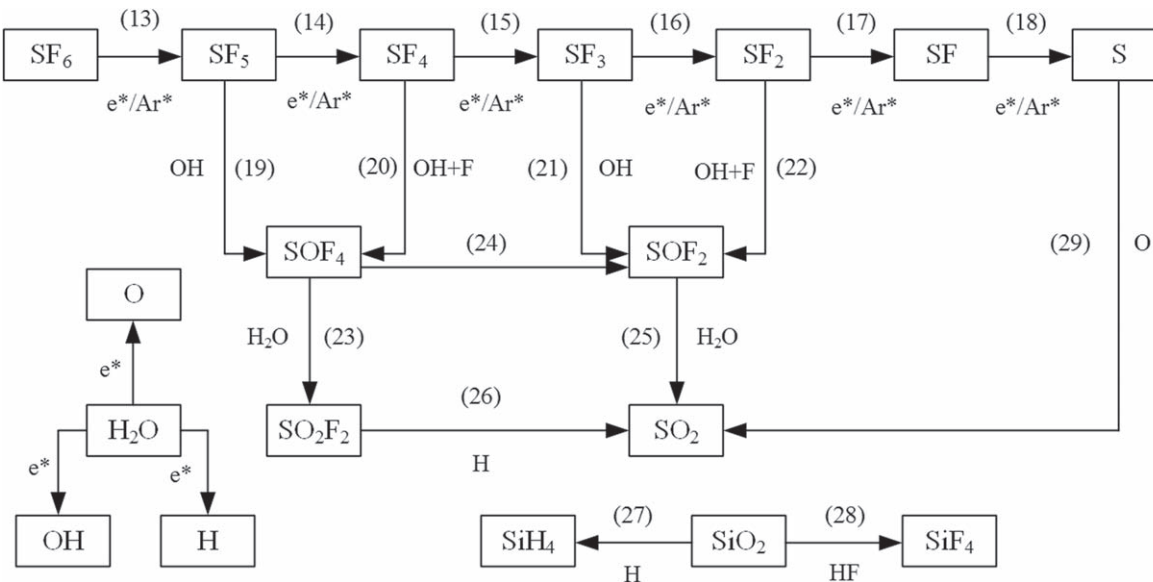
Furthermore, when H₂O concentration reached 0.75%, the highest concentration of 5554.3 ppm was obtained. When the H₂O concentration was lower, most of the H₂O molecules collide with free electrons to generate OH and H radicals (shown in (5)). Those active radicals generated SO₂F₂ easily, so the SO₂F₂ concentration climbed up with the H₂O concentration. However, most H₂O existed in the form of molecules as the increment of water vapor concentration, which has an adverse effect on SO₂F₂. Finally, SO₂F₂ decreased.

There is a great correlation between SO₂ concentration and H₂O concentration. As the water vapor concentration increased from 0.1% to 2%, SO₂ concentration increased beyond threefold and became the highest product among those four products. This was consistent with previous work. In [31], Zhang *et al* compared the SO₂ production of

SF₆/Ar/O₂ and SF₆/Ar/H₂O systems. The results showed that the selectivity of SO₂ in the latter system was much higher than that of the former. Furthermore, in [40], Zeng *et al* also reported that the addition of water vapor was beneficial to the formation of SO₂. As H₂O concentration increased from 0 to 3000 ppm, the production of SO₂ increased by more than 10 times. Actually, this effect is helpful for the treatment of the exhaust gas because SO₂ is soluble in lye. Plenty of H radicals were consumed by the packing material and glass barriers (equations (27) and (28)). Equation (29) shows that more O radicals were produced with the increment of water vapor concentration, which contributed to the formation of SO₂. At the same time, the concentration of SOF₂ and SO₂F₂ gradually decreased, indicating that SO₂ may be a secondary product of SOF₂ and SO₂F₂ (equations (25) and (26)).

Figure 6(b) displays the distribution of four products' selectivity as a function of water vapor concentration. Similar to figure 5(a) the selectivity of SOF₄ ranged from 0.05% to 4.51%, which was always the lowest. This distribution means that SOF₄ was the most unstable product of this environment, which could not exist in a large amount. Furthermore, SOF₂ and SO₂F₂ were relatively stable, since the selectivity of the two products did not change much under different H₂O concentration conditions. Selectivity of SOF₂ and SO₂F₂ was similar. SO₂F₂ exhibited a higher selectivity due to its higher stability compared with SOF₂. In addition, SO₂ was extremely sensitive to H₂O concentration. When the water vapor concentration exceeded 0.25%, it has the highest selectivity among those four products. There are two reasons accounting for this result. Firstly, SO₂ has a superior stability as a final product. Besides, H₂O concentrations exhibited a very positive influence on the generation of SO₂. All the potential SF₆ degradation paths were summarized in figure 7 and the reaction equations were summarized in table 2.

Figure 8 presents the product concentration and selectivity as a function of SF₆ concentration at 1% H₂O. Higher SF₆ concentration was accompanied by higher products concentration since more SF₆ molecules were degraded under higher SF₆ inlet concentrations. SOF₄ concentration was extremely low (<100 ppm) when the concentration of SF₆

Figure 7. SF₆ degradation paths.

was not more than 2%, but its concentration raised to 13 218.6 ppm (the highest value) as the concentration of SF₆ further increased. Meanwhile, SO₂F₂ increased as SF₆ concentration increased, while SOF₂ concentration remained relatively stable when SF₆ concentration was higher than 1%.

However, the selectivity of these products changed distinctly compared with figure 6(b). The selectivity of SOF₄ was the lowest when SF₆ concentration was lower than 2%. In contrast, as the SF₆ inlet concentration increased to 8%, SOF₄ became the most abundant product. SO₂ also dramatically changed as its selectivity was significantly influenced by SF₆ inlet concentration. Although SOF₂ and SO₂F₂ were still keeping stable during this process, it should be noted that the selectivity of SO₂F₂ was much higher than that of SOF₂.

According to the previous analysis, SOF₄ can be generated in large quantities. However, SOF₄ would continue to react accompanying with a series of other compounds due to the further addition of H₂O molecules, thereby reducing its concentration. However, when the concentration of SF₆ reached 4% or higher, the H₂O content was relatively lower, which caused most SOF₄ to lack the raw materials for further reactions, resulting in an increment of SOF₄ concentration.

When the concentration of SF₆ was 1%, the concentration of SOF₂ was only 154.2 ppm, which was consistent with the above inference, because SOF₂ has a similar reaction path with SOF₄, except that SOF₄ can react with H radical to form SOF₂. Thus, SO₂ with relatively surplus H₂O can be generated easily, resulting in a lower SOF₂ concentration. Therefore, the concentration change of SOF₂ is ahead of the concentration change of SOF₄, where a higher concentration has already achieved when the concentration of SF₆ is 2%. Therefore, the concentration range of the SF₆ is not as large as further increased SF₆ concentration, which indicated that the SOF₂ concentration was not influenced by SF₆ concentration variation, when SF₆ was excessive (>2%). It can be noted from equations (21), (22), (24), and (25) that the number of

decomposed SF₆ molecules increased as the increased SF₆ concentration, but the number of SF₂ and SF₃ did not definitely increase, because when the concentration of SF₆ is low, the same SF₆ molecule can be subjected to multiple collisions and multiple decompositions, thereby generating more SF₂ and SF₃, but the averaged number of collisions per SF₆ molecule will decrease upon the increased number of SF₆ molecules in the system. It will increase the number of SF₄ and SF₅, and reduce SF₂ and SF₃. Eventually, the produced SOF₂ does not increase with the increment of SF₆.

The concentration of SO₂F₂ increased with the increased SF₆ concentration. Firstly, a rapid increase in the concentration of SOF₄ will provide sufficient feedstock to form it. Secondly, the relative content of H₂O will be insufficient for the increased concentration of SF₆, which will limit the consumption path of SO₂F₂. Finally, SO₂F₂ concentration increased due to its stable chemical property. Therefore, as the SF₆ concentration increased from 1% to 8%, the concentration of SO₂F₂ ranged from 385.6 ppm to 11 014.8 ppm.

When the SF₆ concentration increased from 1% to 2%, the SO₂ concentration increased from 1686.7 ppm to 7832.6 ppm. SO₂ is a relatively stable product combined with the previous analysis. When the concentration of SF₆ was doubled, four times of concentration was achieved. However, with the augment of SF₆ concentration, the growth rate of SO₂ production gradually decreased. Finally, when the concentration of SF₆ was 8%, the concentration decreased slightly. This may be due to the fact that the increment of SF₆ led to the decreased SOF₂ concentration and increased SO₂F₂ concentration, while SOF₂ is the raw material for SO₂ generation. In addition, the SO₂F₂ augment will increase the concentration of HF in the system, which also has an inhibitory effect on SO₂ formation.

The performance of different products under different pre-heating temperatures was studied, as shown in figure 9. It can be clearly seen that SOF₄ was positively correlated with

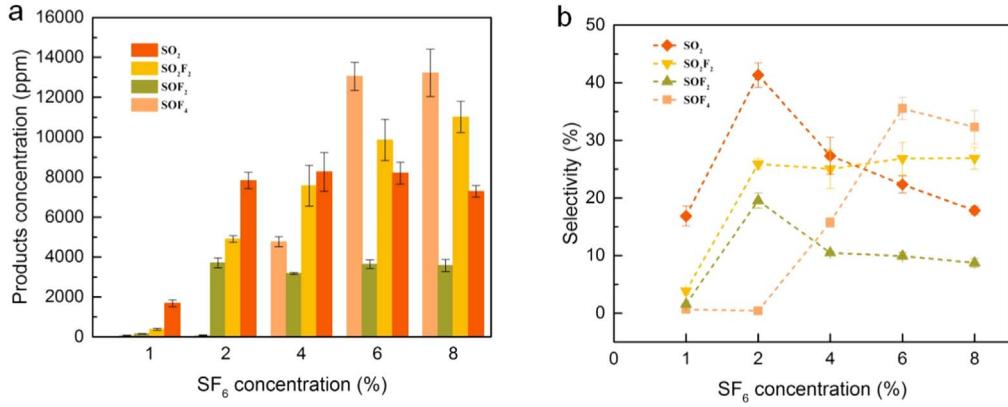


Figure 8. (a) Product concentration under different SF₆ inlet concentrations (1% H₂O, 100 W, 150 ml min⁻¹), (b) product selectivity under different SF₆ inlet concentrations (1% H₂O, 100 W, 150 ml min⁻¹).

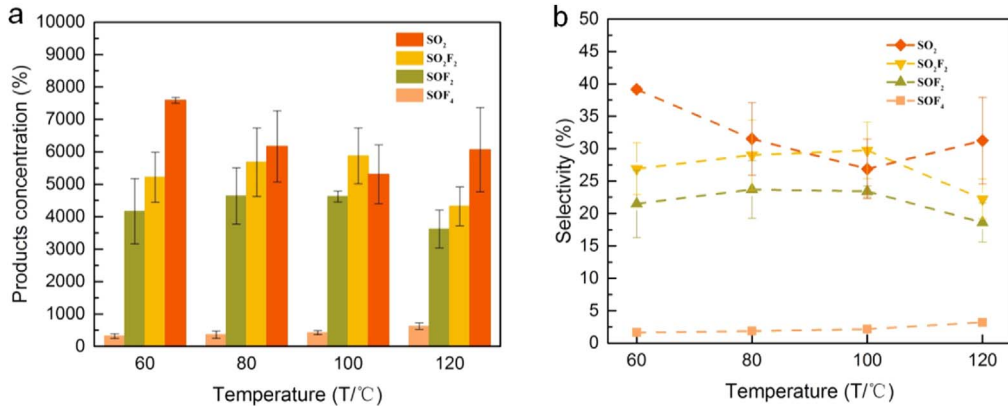


Figure 9. (a) Product concentrations at different pre-heating temperatures (2% SF₆ + 1% H₂O, 100 W, 150 ml min⁻¹), (b) product selectivity at different pre-heating temperatures (2% SF₆ + 1% H₂O, 100 W, 150 ml min⁻¹).

temperature. Its concentration increased from 318.5 ppm at 60 °C to 624.2 ppm at 120 °C. However, pre-heating temperature on the product resulted in much lower selectivity of SO₂ compared with the un-preheated condition.

Only SOF₄ and SO₂ showed different trends from the previous one, according to the influence of temperature on the products. Among them, SOF₄ increased with the temperature. Referring to its generation and consumption paths, it can be found that the increment of temperature may have a certain inhibitory effect on its further transformation. SO₂ decreased first and then raised with the temperature, which may be associated with the stability of SO₂ and its raw materials at different temperatures. Reference [17] studied the methanol conversion product distribution characteristics at different pre-heating temperatures. As pre-heating temperature increases, some products changed significantly. However, [41] pointed out that the temperature changes below 400 °C would not influence SF₆ degradation. Therefore, the mechanism for the temperature effect on the products is still unknown. Finally, it can be noted that the increment of temperature causes a slight decrease in the total amount of these four products, the reduced portion may be converted into other compounds.

In our previous work, we have investigated the effects of three parameters on SF₆ degradation. Water molecules could

participate in the physical and chemical reactions of the plasma region, which deeply influences the SF₆ removal efficiency and product distribution. Primarily, the addition of water vapor significantly improved the processing efficiency of SF₆, the degree of improved efficiency varied as the water vapor concentration changed. The analysis demonstrated that the effect of water vapor concentration was subject to specific conditions, so the position of the optimal equilibrium point is not fixed. In addition, electrical signals and emission spectra have shown that the entire process was mainly influenced by the participation of water molecules in chemical reactions during the SF₆ process, and the changes in electrical parameters were negligible. The water vapor concentration mainly exhibited an influence on the selectivity of SOF₄ and SO₂, which indicated that adjusting its concentration should be considered preferentially where the product treatment is mainly concerned. The main change induced by the increment of SF₆ concentration was the increased stability and primary products such as SO₂F₂ and SOF₄. This may be due to the increased energy utilization. The pre-heating temperature further increased the efficiency of DBD treatment of SF₆ and only affected the production of SOF₄. Therefore, pre-heating the mixed gas is a feasible method under the high DRE demand condition. In summary, the proper water vapor concentration and pre-heating temperature play a great crucial

Table 3. Products and parameters relationship.

Product	Water vapor concentration	SF ₆ inlet concentration	Pre-heating temperature
SOF ₄	✓	✓	✓
SOF ₂		✓	
SO ₂ F ₂			
SO ₂	✓		✓

role in the improvement of the DRE; but for EY, the inlet concentration of SF₆ is the most important.

Finally, the relationship between the products and the parameters were defined in table 3. ✓ indicates that a particular product is susceptible to a particular parameter.

4. Conclusions

In this study, the degradation of SF₆ in a packed bed plasma reactor was investigated comprehensively. Removal efficiency and products selectivity have been discussed under different parameter conditions, including the water vapor concentration, SF₆ inlet concentration and pre-heating temperature. The best promoted effect was achieved by 1% H₂O when the water concentration was in the range of 0.1%–2%, and its DRE reached 95.7% at 2% SF₆. Under 100 °C pre-heating, this value further reached 98.7%. Therefore, an appropriate amount of moisture addition and pre-heating temperature could increase the removal efficiency of SF₆. Moreover, the EY at different initial concentrations demonstrated that higher SF₆ concentration had a favorable effect on EY. The current waveform of the PBR tube revealed that the presence of moisture influenced the filament discharge process within the reactor. The emission spectrum data suggested that water molecules participated in reactions, which confirmed that the dissociation of H₂O molecules consumed a certain amount of discharge energy. Furthermore, the variation of the four products was also presented by adjusting the above three parameters. Among the four products, the negligible influence of water vapor concentration, initial concentration of SF₆ and pre-heating temperature on most stable SO₂F₂ was achieved; although SO₂ is also a relatively stable product, its concentration is greatly affected by water vapor concentration and pre-heating temperature; SOF₂ is greatly affected by the initial concentration of SF₆; SOF₄ as the most unstable product was affected by all the three parameters.

The inlet concentration of SF₆ has the greatest influence on EY, which should be considered preferential when higher EY was needed. Pre-heating and water vapor can result in complete degradation of SF₆, and it is also an effective way to promote SF₆ abatement. The distributions of the products indicated that certain products can be obtained by manipulating experimental conditions for subsequent further processing. In addition, DBD is only suitable for processing SF₆ gas under low concentrations and flow rates due to the limitation of existing technologies. Subsequent studies can be carried out from these two aspects.

This article provides a deeper understanding of the performance of PBRs in SF₆ abatement and makes a preparation for its large-scale application.

Acknowledgments

This study is funded by National Natural Science Foundation of China (No. 51777144) and State Grid Science and Technology Project (SGHB0000KXJS1800554).

References

- Xiao H Y 2018 Studies on SF₆ degradation by atmospheric dielectric barrier discharge plasma and its combination with catalysts *PhD Thesis* Chongqing University (in Chinese)
- Li Y et al 2019 *Chem. Eng. J.* **360** 929
- Li Y et al 2019 *J. Hazard. Mater.* **368** 653
- Rabie M and Franck C M 2018 *Environ. Sci. Technol.* **52** 369
- Li Y et al 2019 *Corros. Sci.* **153** 32
- Li Y et al 2018 *Ind. Eng. Chem. Res.* **57** 5173
- Li Y L et al 2019 *IEEE Access* **7** 83994
- Kashiwagi D et al 2009 *Ind. Eng. Chem. Res.* **48** 632
- Kashiwagi D et al 2009 *J. Colloid Interface Sci.* **332** 136
- Chen S H et al 2019 *J. Fluor. Chem.* **217** 41
- Huang L et al 2008 *J. Environ. Sci.* **20** 183
- Song X X et al 2009 *J. Hazard. Mater.* **168** 493
- Lee H M, Chang M B and Wu K Y 2004 *J. Air Waste Manag. Assoc.* **54** 960
- Tsai C H and Shao J M 2008 *J. Hazard. Mater.* **157** 201
- Mok Y S and Kim D H 2011 *J. Korean Phys. Soc.* **59** 3437
- Wang X X 2009 *High Volt. Eng.* **34** 1 (in Chinese)
- Wang L et al 2016 *Green Chem.* **18** 5658
- Jiang N et al 2019 *J. Hazard. Mater.* **369** 611
- Jiang N et al 2018 *Chem. Eng. J.* **350** 12
- Chang C L and Lin T S 2005 *Plasma Chem. Plasma Process.* **25** 227
- Obradović B M, Sretenović G B and Kuraica M M 2011 *J. Hazard. Mater.* **185** 1280
- Zhang X X et al 2017 *Crit. Rev. Environ. Sci. Technol.* **47** 1763
- Zhang X X et al 2018 *IEEE Trans. Plasma Sci.* **46** 563
- Kim H H et al 2005 *IEEE Trans. Ind. Appl.* **41** 206
- Cui Z L et al 2019 *Plasma Chem. Plasma Process.* **40** 43–59
- Chen H L et al 2008 *Ind. Eng. Chem. Res.* **47** 2122
- Butterworth T, Elder R and Allen R 2016 *Chem. Eng. J.* **293** 55
- Michielsen I et al 2017 *Chem. Eng. J.* **326** 477
- Chen H L et al 2008 *IEEE Trans. Plasma Sci.* **36** 509
- Zhang X X et al 2018 *J. Hazard. Mater.* **360** 341
- Zhang X X et al 2018 *IEEE Access* **6** 72748
- Zhang X X et al 2018 *Proc. CSEE* **38** 937 (in Chinese)
- Tang J et al 2013 *Proc. CSEE* **33** 211 (in Chinese)
- Chen D C et al 2019 *IEEE Trans. Device Mater. Rel.* **19** 473
- Li Y et al 2019 *High Volt.* **4** 12
- Luo H Y, Ran J X and Wang X X 2012 *High Volt. Eng.* **38** 1070 (in Chinese)
- Tian Y et al 2019 *RSC Adv.* **9** 34827
- NIST Atomic Spectra Database Lines Data https://physics.nist.gov/PhysRefData/ASD/lines_form.html
- Xu S J, Whitehead J C and Martin P A 2017 *Chem. Eng. J.* **327** 764
- Zeng F P 2014 Decomposition characteristics of SF₆ under spatial over-thermal fault and the influence mechanism of trace H₂O *PhD Thesis* Chongqing University (in Chinese)
- Cui Z L et al 2020 *J. Phys. D: Appl. Phys.* **53** 025205